International Journal of Research in Engineering and Science (IJRES)
ISSN (Online): 2320-9364, ISSN (Print): 2320-9356
www.ijres.org Volume 11 Issue 7 ǁ July 2023 ǁ PP. 70-78

Influence of infinitesimal shear on invanriantsand the stress tensor components of a cylindrical tube: Application to three models

Jérémie Gaston SAMBOU [1*], Edouard DIOUF [2]

Laboratory of Mathematics and Applications University Assane Seck of Ziguinchor, BP 523 Senegal.

Abstract:
In this research work we have proposed to study a hollow cylindrical tubular structure subjected to an infinitesimal anti-plane shear. we used three energy functions of deformation which is logarithmic, power and exponential form re- spectively to determine the shear solution. The calculations allowed us with certain conditions to find a logarithmic solution of the shear in the three mod- els. The numerical simulation of the anti-plane shear shows that the Diouf-Zidi model give the greatest shear followed by the Knowles-Sterberg shear while the Defino model records the lowest shear. And as a consequence, the principal com- ponents of the Cauchy stress tensor are constant functions whereas the other components of this tensor and the invariants have a behavior which increases on the scale of the arterial radius. Finally, we find that indity component of the Cauchy stress tensor has a strong influence on the behavior of an isotropic incompressible tube subjected to an infinitesimal anti-plane shear.

Keywords:
Anti-planar shear, Incompressible transformation, Isotropic energy function,Elementary invariants, Cauchy stress tensor.

Date of Submission: 29-06-2023 Date of acceptance: 09-07-2023

I. Introduction

The study of shearing of elastic and incompressible materials has always been the subject of special attention in the study of mechanical systems [1]. In the study of mechanical fracture, following the example of anti-planar shear has been of particular interest to better understand these mechanical systems. Sim- ple shear deformations, for which the displacement gradient is constant, are sustainable both in the linear and nonlinear theory. So that necessary and sufficient conditions on the strain energies for homogeneous isotropic nonlinear elastic materials which do allow antiplane shear were obtained in Knowles for further contributions in the compressible case [2].

In the linear transversely isotropic elasticity, a study the deformation of a cir- cular infinite hollow cylinder, whose inner face is fixed, while its outer surface is subject to a constant axial surface traction[3]. In isotropic linear elasticity, the solution of this problem is just a state of anti-plane axial shear. The autors show that it is possible to use an axial tension field to generate an azimuthal shear deformation. they show that this fact suggests to use anisotropy to design some elastic machines which can combine different deformation modes.

Other authors [4] have shown that this characterization of materials is closely related to the nature and form of the energy function. This characterization remains less obvious in nonlinear elasticity.

Other studies have focused on the effect of shear stress in generated by a fluid in a tubular structure [5]. Their study showed that in the renal tube reduced fluid shear stress down-regulated the levels of megalin receptors, thereby reducingthe renal distribution of albumin nanoparticles.

To describe the anisotropic hyperelastic mechanical behavior of a mechanical structure, it is still useful to use deformation energy functions in form poly- nomial, exponential, power or logarithmic. These energy potentials have been established as part of a phenomenological approach that describes the macro- scopic nature of the material.

The study of the anti-plane shear of a cylindrical tubular structure and its influ- ence on invariants and non-zero components of the Cauchy stress tensors with a three-way application of energy functions will be our contribution in the biome- chanical modeling, we study a smooth hollow cylindrical structure subjected to anti-planar shear incompressible isotropic case by application to energy poten- tial.

After the calculation of the anti planar-shear of the three models of our study, The elementary invariants and the non-zero components of the Cauchy stress tensor and these founded shears are

simulated and analyzed with some bound- ary conditions which are given on the parameters according to whether that theradius increases.

II. Formulation of the problem

Consider a continuous material body. the whole of the particles of this body occupies, every moment, an open and connected domain or connected by arc of the physical space. The geometric domain is a hollow cylinder composed of an elastic, isotropic material with an inner surface bounded by a rigid cylinder and an outer surface subjected to axial shear. In a cylindrical coordinate sys- tem, let's consider a point M which, in the undeformed configuration has the components (R, Θ, Z) and the deformed configuration (r, θ, $\varkappa$). The kinematicsof deformation is described in [6] by:

$r = r(R); \theta = \Theta; \varkappa = Z + \omega(R)$ (1)

which translates for axial shear, a combined deformation of the tube: radial with $r(R)$ and longitudinal or shear anti plan with $\omega(R)$.

With clearly defined boundary conditions on the inner R_i and outer R_e radius

[7]. According to (1), we find the following deformation gradient tensor:

$$\mathbf{F} = \begin{pmatrix} r' & 0 & 0 \\ 0 & \frac{r}{R} & 0 \\ \omega' & 0 & 1 \end{pmatrix} \tag{2}$$

where r' and ω' are respectively the derivatives with respect to R of r and ω.
From the deformation gradient, we can calculate:
The right Cauchy-Green tensor in the case of a representation in Lagrangian configuration defined by:

$$\mathbf{C} = \mathbf{F}^T\mathbf{F} = \begin{pmatrix} r'^2 + \omega'^2 & 0 & \omega' \\ 0 & \frac{r^2}{R^2} & 0 \\ \omega' & 0 & 1 \end{pmatrix} \tag{3}$$

But also the left Cauchy-Green tensor in the case of a representation in Eulerian configuration defined by:

$$\mathbf{B} = \mathbf{F}\mathbf{F}^T == \begin{pmatrix} r'^2 & 0 & r'\omega' \\ 0 & \frac{r^2}{R^2} & 0 \\ r'\omega' & 0 & 1 + \omega'^2 \end{pmatrix} \tag{4}$$

It should be noted that these two re-representation are equivalent and they are confused in the case of an infinitesimal deformation.
It's follow the first three elementary invariants of $\mathbf{B}$ or $\mathbf{B}$ given by:

$$\begin{aligned} I_1 = tr(\mathbf{C}) = tr(\mathbf{B}) = r'^2 + \left(\frac{r}{R}\right)^2 + \omega'^2 + 1; \\ I_2 = tr(\mathbf{C}^*) = tr(\mathbf{B}^*) = r'^2 + \left(\frac{r}{R}\right)^2 (1 + \omega'^2) + \left(\frac{r}{R}\right)^2; \\ I_3 = det(\mathbf{C}) = det(\mathbf{B}) = \left(\frac{rr'}{R}\right)^2. \end{aligned} \tag{5}$$

Where tr defines the *trace* operator, *det* the *determinant* operator and $\mathbf{C}^*$ and $\mathbf{B}^*$ are respectively the adjoints of the tensors $\mathbf{C}$ and $\mathbf{B}$ which are defined by:

$$\mathbf{C}^* = det(\mathbf{C})\mathbf{C}^{-1}; \qquad \mathbf{B}^* = det(\mathbf{B})\mathbf{B}^{-1}. \tag{6}$$

It should be noted that the elementary invariants allows us to obtain the energy potential W also called the deformation energy function which is a function of these invariants ($W(I_1, I_2, I_3)$). This function translates the mechanical and/or thermodynamic behavior of the material.
To translate the reaction of the material when it is submited to stresses which it undergoes, we introduce a tensor $\boldsymbol{\sigma}$ called Cauchy stress tensor.
The stress tensor of Cauchy is given in [8]:

With

$$\begin{aligned} \beta_0 &= 2I_3^{-1/2}\left(I_2W_2 + I_3W_3\right) \\ \beta_\varepsilon &= 2I_3^{-1/2}W_1 \\ \beta_{-\varepsilon} &= -2I_3^{1/2}W_2. \end{aligned} \tag{8}$$

The $W_{i=1,2,3}$ are the partial derivatives of W with respect to the invariants i.e $W_i = \partial W/\partial I_i$.
In relation (7), the right Cauchy -Green tensor can be replaced by the left Cauchy Green tensor.
The expression of pressure P is given by:

$$P = 2I_3^{-1/2}\left(I_2W_2 + I_3W_3\right) \tag{9}$$

To write equilibrium equations, it is necessary to isolate a material domain and to apply to it the fundamental principle of dynamics. So then in the absence of volume forces, the equilibrium equation is given by:

$$div(\boldsymbol{\sigma}) = 0. \tag{10}$$

According to a study carried out in [6], the equations of equilibria are reduced to:

$$\begin{aligned} \frac{\partial \sigma_{rr}}{\partial r} + \frac{\sigma_{rr} - \sigma_{\theta\theta}}{r} &= 0 \\ \frac{\partial \sigma_{rr}}{\partial r} + \frac{\sigma_{rz}}{r} &= 0. \end{aligned} \tag{11}$$

By choosing as a condition to the limits on the inside radius R_i in [6] and outside radius R_e in [9] of the tube:

$$\begin{aligned} r(R_i) = R_i; \qquad & \omega(R_i) = 0 \\ \sigma_{rr}(R_e) = 0; \qquad & \sigma_{rz}(R_e) = \sigma_0. \end{aligned} \tag{12}$$

where σ_0 is an initial constraint.
Starting from this previous reduction and with the necessary condition of shearing in the condition of incompressibilité i.e $r = R$ and $I_3 = 1$, add with some calculations and a double integration gives us the solution of the anti plane shear ω which becomes:

$$\omega = \frac{R_e\sigma_0}{W_1 + W_2} log(R) + C_0. \tag{13}$$

where C_0 is an integration constant.
Regarding the derivative of the anti-plane shear ω, we consider its infinitesimal rate of an increasing radius of the order 10^{-3}, which means that I_1 is close to the value 3 but will never be equal to 3 because this rate of change is always greater than zero.

3 Application

3.1 Model of Diouf-Zidi

Let's consider now the Diouf-Zidi model energy function defined in [10] by:

$$W = a_1 (I_1 - 3) + a_2 (I_2 - 3) + a_3 \left[\left(I_3^{1/p} - 1 \right) + (2 - p)(I_3 - 1) \right] + a_4 \frac{2-p}{1+p} log(I_3); \tag{14}$$

where p is a positive real.
From this previous energy function, the condition of incompressibility yields us:

$$W = a_1 (I_1 - 3) + a_2 (I_2 - 3). \tag{15}$$

Relation (15) allow us to obtain the solution of the anti planar shear in the case of a Diouf-Zidi model incompressible material given by:

$$\omega(R) = \frac{R_e \sigma_0}{a_1 + a_2} log(R) + C_0. \tag{16}$$

Here we see that the Diouf-Zidi modelin incompressible allow us to obtain a a logarithmic solution of the anti-planar shear.

3.2 Knowles-Sternberg Model

We consider here to be in the case of a transformation in anti-plane mode the Knowles-Sternberg energy function by a power law [11]:

$$W = \frac{\mu}{2} \left(1 + \frac{b}{n} (I_1 - 3) \right)^n, \tag{17}$$

where μ and b are material parameters and n a strictly positive power.
Depending on the power, the local equations of movement are of a nature respectively elliptical, parabolic or elliptique-hyperbolic when the power n is respectively $> 1/2$, $= 1/2$ or $< 1/2$.
With the absence of the second invariant, the partial derivative correspondand becomes zero.
the computation of the partial derivative with respect to the second invariant gives:

$$W_1 = \frac{\mu b}{2} (I_1 - 3)^{n-1}, \tag{18}$$

The expression (18) allows us to have the general expression of the anti planar shear for the Knowles-Sternberg model.

$$\omega = \frac{2 R_e \sigma_0}{\mu b} (I_1 - 3)^{1-n} log(R) + C_0. \tag{19}$$

It should be noted that the shear will always be defined in the case of a purely longitudinal incompressible deformation because $I_1 - 3 \neq 0$.

So if we assume the case where the equations of motion are elliptical with $n = 1$, we finally find:

$$\omega(R) = \frac{2 R_e \sigma_0}{\mu b} log(R) + C_0. \tag{20}$$

So the power model of Knowles-Sternberg gives us a logarithmic solution of the anti-planar shear with certains conditions on the power in incompressible.

3.3 Delfino Model

We have defined in the case of a transformation in anti-plane mode a energy function by an exponential law [12]:

$$W = \frac{\beta_1}{2}\left[exp\left(\frac{\beta_2}{2}(I_1 - 3)\right) - 1\right], \tag{21}$$

with β_1 and β_2 are material parameters.
With also the absence of the second invariant, the partial derivative correspondand is zero.
the computation of the partial derivative with respect to the second invariant gives then:

$$W_1 = \frac{\beta_1\beta_2}{4}exp\left(\frac{\beta_2}{2}(I_1 - 3)\right), \tag{22}$$

The expression (22) allows us to have the general expression of the anti planar shear for the Delfino Model.

$$\omega = \frac{4R_e\sigma_0}{\beta_1\beta_2}exp\left(-\frac{\beta_2}{2}(I_1 - 3)\right)log(R) + C_0. \tag{23}$$

With the condition that I_1 is close to the value 3, we obtain a simple expression of shear of the Delfino:

$$\omega(R) = \frac{4R_e\sigma_0}{\beta_1\beta_2}log(R) + C_0. \tag{24}$$

As for the power model of Knowles-Sternberg, the Delfino model which has an exponential form gives also a logarithmic solution of the anti-planar shear with certains conditions in incompressible.

Remark:
We find that the anti-plane shear solutions obtained for these three models are equivalent for certain conditions.
And in the case where we have : $4(a_1 + a_2) = 2\mu b = \beta_1\beta_2$, these solutions become identical.

4 Numerical simulation and interpretation

In this paragraph, we proceed to the simulation of some of the expressions found in the previous sections like anti-plane shear, elementary invariants and non-zero

components of the stress tensor for the three models studied previously.
To do this work, we will consider the shear solution obtained for each model in order to see its influence on the other components derived from it and then to better see the behavior of the shearing and its influence on the invariants, the different components of the Cauchy stress tensor and also it influence on the pressure.we assume the hypothesis of the ifinitesimal variation of the radius
To finish, we also consider the conditions that initially there is no shearing with an initial state of stress. These boundary conditions with the hardware parameters used are defined in the following table

parameters	values
a_1	44.28 [KPa] [13,14]
a_2	21.79 [KPa] [14]
β_1	44.28 [KPa] [14]
β_2	16.7 [KPa] [14]
μ	44.28 [KPa] [14]
b	3.58 [KPa] [14]
σ_0	12.399 [KPa] [14]
R_e	0.00482 [14]

1.1 Anti planar shears and Invariants

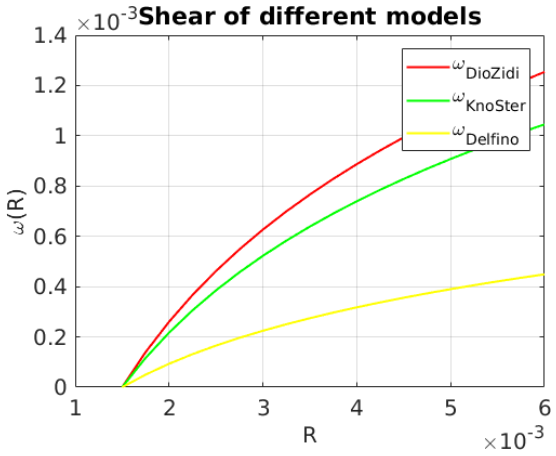

As the graph shows, initially, all three shears are zero. When the radius begins to grow, the shear rate found for the Diouf-Zidi model grows faster followed by the shear of the Knowles-Sternberg model with the difference of the order of 0.2 for radius of 6×10^{-3} and then by the delfino model with a difference of around 0.8 for for a radius of 6×10^{-3}.
With our study hypothesis, we have the Diouf-Zidi model which records greater shear followed by the Knowles-Sterberg while the Defino model records the lowest shear.

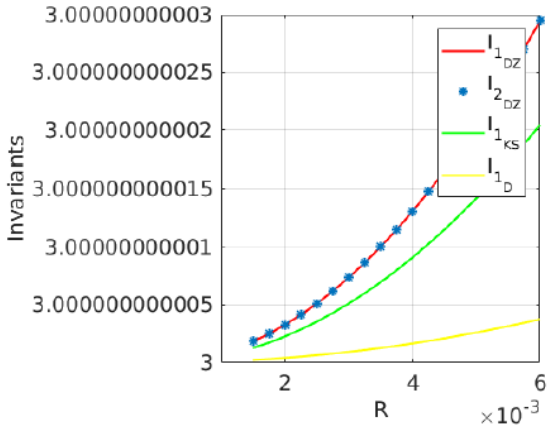

On the arterial radius scale, all the invariants follow a linear behavior which is parallel to the horizontal axis and remain almost identical or even superimpos- able if we stopped at three digits after the decimal point. But in the case where we consider up to twelve digits after the decimal point, we note increasing gaits with the first and the second invariant of the Diouf-Zidi model which are the largest while remaining identical followed respectively by the first invariant of the Knowles-Sternberg model and that Delfino's model.

4.2 The non-zero components of the stress tensor

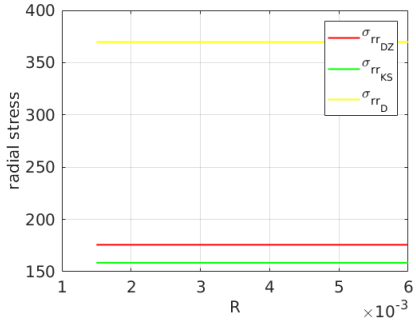

The simulation of the radial component on the arterial radius scale shows that these components follow a linear behavior which is parallel to the horizontal. The shape of the components shows differences in values. The component of the delfino model followed by the Diouf-Zidi model while the Knowles-Sternberg model remains the smallest.
You need to underline that in the case where we consider up to twelve digits after the decimal point, we will see increasing behavior of the three components.

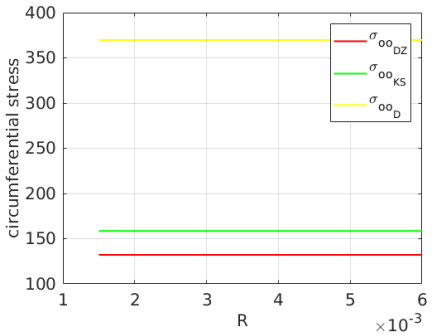

As previously, the simulation of the circumferential component on the arterial radius scale shows that these components follow a linear behavior which is par- allel to the horizontal.The shape of the components also shows differences in values. unlike the observations noted in the case of the radial component, we note the circumferential component of the Delfino model is followed by that of the Knowles-Sternberg model and that that of Diouf-Zidi remains the smallest. Increasing behavior of the three components in the case where we consider upto twelve digits after the decimal point are also observed.

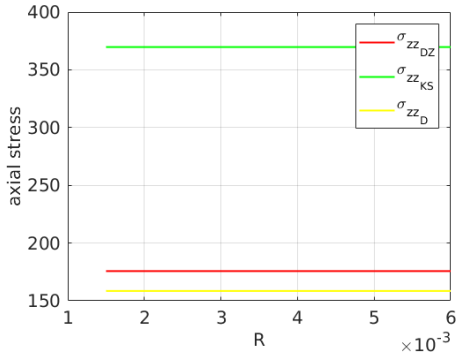

As previously, the simulation of the axial component on the arterial radius scale of the three models shows also that these components follow a linear behavior which is parallel to the horizontal.The shape of the components shows differ- ences in the values. The observations noted in the case of the axial component show that the component of the Knowles-Sterberg is the bigest followed by that of the Diouf-Zidi model and that that of Defino model is the smallest in contrary to the two previous cases.
Increasing behavior of the three components are also observed in the case where we consider up to twelve digits after the decimal point.

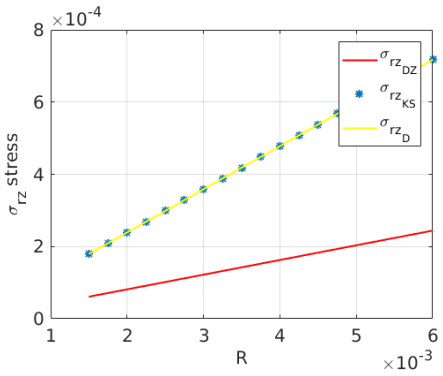

In the case of the component σ_{rx}, we can note a linear behavior of this compo- nent for all the three models during the simulation, nevertheless this behavior does not remain any more parallel to the horizontal axis. A perfect resemblance on the one hand and difference on the other hand ac- cording to the models are observed. As we can see at the graph level, there is a perfect resemblance of behavior of this component between the Knowles- Sternberg model and the model of Delfino which remain larger with increasing gaits. The Diouf-Zidi model obtains the smallest value by having an increasing pace with a divergence of values observed compared to the other two models when the radius also increases.
The same behavior is exactly observed at the level of the three models for the component σ_{xr}.

Remark:
It should be remembered here that in the case where one considers up to twelve digits after the decimal point, the paces of all the simulated components give an increasing behavior while preserving the same orders of magnitude. But when we limit ourselves to the scale of the arterial radius, that is mean to four digits after the decimal point only the shear $\omega(R)$ and the components σ_{rx} and σ_{xr} of the Cauchy stress tensor give an increasing pace. The main components are linear gears parallel to the abscissa axis.
Another observation that we made is that there is not an absolute proportion- ality relationship between our three models because the component of a model can be the smallest in the case of an expression and become the largest in the case of another expression studied.
The simulation allowed us to see that the main component of the stress tensor $\beta_0\mathbf{1}$ has a strong influence on the behavior of the cylindrical tubular material subjected to an increasing anti-plane shear compared to the radius of the in- compressible tube.

V. Conclusion

In this work of modeling a hollow cylindrical tubular structure subjected to an infinitesimal anti-plane shear, we have used a fundamental solution of this shear obtained in previous studies in the case of an isotropic material in incompressible. To do that, we used three energy functions of deformation of logarithmic, power and exponential form respectively.

In the first part reserved for calculations, this study allowed us to determine the integral solution of the shear for each models, a solution which is always of the logarithmic form for a certain choice on the power in infinitesimal transformation. We also noticed that for a certain choice on the material parameters, these solutions become identical.

For the part reserved for numerical simulation, the anti-plane shear solution with our study hypothesis, shows that the Diouf-Zidi model give the greatest shear followed by the Knowles-Sterberg shear while the Defino model records the lowest shear. As a consequence, a highlighted result is that the principal components of the tensor of constraint are constant functions of R whereas the other components of this tensor and the invariants have a behavior which in- creases as a function of R on the scale of the arterial radius .
this study allowed us to prouve that the term of the indity component of the
Cauchy stress tensor has a strong influence on the behavior of the cylindrical tubular material when it is subjected to an anti-plane shear with an increasing radius in arterial scale of an incompressible and isotropic tube.

References

[1]. R. S. Rivlin, M. F. Beatty, "Dead loading of a unit cube of compressible isotropic elastic material". Z Agnew Math Phy. 954-963, (2003).

[2]. J.K. Knowles, "The finite anti-plane shear field near the tip of crack for a class of incompressible elastic solids", Inter.J.Fracture, 13, 611, (1977).

[3]. F. Grine, G. Saccomandi, M. Arfaoui. "Elastic machines: A non standard use of the axial shear of linear transversely isotropic elastic cylinders". https://doi.org/10.1016/j.ijsolstr.2019.08.025.

[4]. J. K. Knowles, "On note on anti-plane shear for compressible mateials in finite elastostatics, J. Austral. Math. Soc. Ser. B 19, 1-7, (1977).

[5]. Y. Xu, S. Qin, Y. Niu, T. Gong, Z. Zhang, Y. Fu, "Effect of fluid shear stress on the internalization of kidney-targeted delivery systems in renal tubular epithelial cells". Acta Pharmaceutica Sinica B, https://doi.org/10.1016/j.apsb.2019.11.012.

[6]. J. G. Sambou and E. Diouf., "Analysis of the antiplane shear of certain materials". International Journal of Scientific Engineering Research Vol 9, Issue 3 (2018).

[7]. R.W.Ogden, "Non-linear elastic deformations", Ellis Horwood, Chichester, (1984).

[8]. C.Truesdell, W.Noll, The non-linear field theories of mechanics, Hand- buchder physic, III/3, S. Flugge, ed., Springer-Verlag, Berlin, (1965).

[9]. E Diouf, Effects of prestress on a hyperelastic, anisotropic and compres- sible tube, Inter. Journal of Sci and Eng Research, Vol 6, 1672-1677, (2015).

[10]. E.Diouf, M. Zidi,Finite azimuthal shear motions of a transversely isotropic compressible elastic and prestressed tube, Inter.J.of Eng. Sci., 43, 262- 274, (2005).

[11]. C. Stolz, "Milieux Continus en transformations finies, Hyperelasticité, Rupture, Elastoplasticité", Ed. Ecole Polytechnique, (2010).

[12]. M. Zulliger, N. Stergiopulos, "Structural strain energy function applied to the ageing of human aorta", J. Biomech., 40 (14), 3061-9, (2007).

[13]. A. Delfino, N. Stergiopulos, J. E. Jr Moore, J. J. Meister, "Residual strain effects on the stress field in a thick wall finite element model of the human carotid bifurcation", Journal of Biomechanics, 30:777-86 (1997).

[14]. I. Masson, P. Boutouyrie, S. Laurent, J. D. Humphrey and M. Zidi, "Me- chanical modeling of in vivo human carotid arteries from non-invasive clinical data. Proceedings of the Artery 8, Ghent, Belgium. Artery Research 2(3), 113 (2008).